Published in final edited form as:
Atmos Environ. 2010 September 1; 44(28): 3422–3431. doi:10.1016/j.atmosenv.2010.06.005.

Quantification of Self Pollution from Two Diesel School Buses using Three Independent Methods

L.-J. Sally Liu[1,2,3,*], **Harish C. Phuleria**[1,2], **Whitney Webber**[3], **Mark Davey**[3], **Douglas R. Lawson**[4], **Robert G. Ireson**[5], **Barbara Zielinska**[6], **John M. Ondov**[7], **Christopher S. Weaver**[8], **Charles A. Lapin**[9], **Michael Easter**[10], **Thomas W. Hesterberg**[11], and **Timothy Larson**[12]

[1] Swiss Tropical and Public Health Institute, Basel, Switzerland [2] University of Basel, Basel, Switzerland [3] Department of Environmental and Occupational Health Sciences, University of Washington, Seattle, WA [4] National Renewable Energy Laboratory, Golden, CO [5] Air Quality Management Consulting, Greenbrae, CA [6] Atmospheric Sciences Division, Desert Research Institute, Reno, NV [7] Department of Chemistry and Biochemistry, University of Maryland, College Park, MD [8] Engine Fuel & Emissions Engineering, Inc., Rancho Cordova, CA [9] Lapin & Associates, Glendale, CA [10] California EnSIGHT, Walnut Creek, CA [11] International Truck and Engine Corporation, Warrenville, IL [12] Department of Civil and Environmental Engineering, University of Washington, Seattle, WA

Abstract

We monitored two Seattle school buses to quantify the buses' self pollution using the dual tracers (DT), lead vehicle (LV), and chemical mass balance (CMB) methods. Each bus drove along a residential route simulating stops, with windows closed or open. Particulate matter (PM) and its constituents were monitored in the bus and from a LV. We collected source samples from the tailpipe and crankcase emissions using an on-board dilution tunnel. Concentrations of PM_1, ultrafine particle counts, elemental and organic carbon (EC/OC) were higher on the bus than the LV. The DT method estimated that the tailpipe and the crankcase emissions contributed 1.1 and 6.8 μg/m^3 of $PM_{2.5}$ inside the bus, respectively, with significantly higher crankcase self pollution (SP) when windows were closed. Approximately two-thirds of in-cabin $PM_{2.5}$ originated from background sources. Using the LV approach, SP estimates from the EC and the active personal DataRAM (pDR) measurements correlated well with the DT estimates for tailpipe and crankcase emissions, respectively, although both measurements need further calibration for accurate quantification. CMB results overestimated SP from the DT method but confirmed crankcase emissions as the major SP source. We confirmed buses' SP using three independent methods and quantified crankcase emissions as the dominant contributor.

Keywords

school bus; self pollution; $PM_{2.5}$; dual tracers; tailpipe; crankcase emissions; cabin air; exposure

[*]Corresponding author: phone: +41-61-461-7525; Fax: +41-61-267-6190; sally.liu@unibas.ch.

Introduction

Over 24 million children in the United States commuting by school buses are likely exposed to exhaust from the buses and other on-road vehicles (U.S. EPA, 2003). Elevated levels of $PM_{2.5}$, PM_{10}, and black carbon (BC) over the background levels were found in 2 Connecticut school buses (Wargo, 2002) and 6 school buses in Los Angeles (LA) (Behrentz et al., 2005; Sabin et al., 2005a; Sabin et al., 2005b). These studies focused on characterizing total in-cabin exposure, which consists of the bus's self pollution and background pollution from other on-road vehicles, re-entrained roadway dust, tire and brake wear, and the urban background pollution (Behrentz et al., 2004). In a recent study in Austin, TX, Rim et al. (2008) observed lower or similar $PM_{2.5}$ and particle counts (PN) in 6 different buses compared to roadway levels. Independent ambient levels are however, not reported. The study also reported 26–60% and 7–43% reduction in bus-cabin $PM_{2.5}$ and PN respectively for those buses which used a crankcase filtration system.

Other studies sought to distinguish the bus's SP from other on-road sources. Solomon et al. (2001) using an Aethalometer to measure BC as a marker for diesel exhaust, reported elevated BC on 4 unoccupied buses navigating in LA, as compared with those in a lead vehicle (LV). However, the actual SP levels were not reported. Our recent study in Seattle examined onboard $PM_{2.5}$ conc. over 43 buses and observed average in-cabin concentrations four and two times higher than ambient and roadway levels respectively. The study reported average SP levels of 7 $\mu g/m^3$ (Adar et al., 2008). Behrentz et al. (2004) injected the tracer sulfur hexafluoride (SF_6) into the tailpipe of 6 diesel school buses driven in LA and estimated 0.01–0.29% of the air inside the cabin was from bus's own exhaust. Wu et al. (1998) used a fuel-based iridium (Ir) tracer to estimate commuters' exposure to tailpipe emissions from the Baltimore metro-buses and reported the soot exposure ($\leq$3 to 82 ng/m^3) as a small fraction of the Baltimore background EC levels. These studies could not estimate levels of PM or BC attributable to the tailpipe because the relation between emission and tracer concentrations was not quantified. With chassis dynamometer testing, Ireson et al. (2004) quantified the PM/tracer ratio in diesel exhaust on one bus and reported 0.22 $\mu g/m^3$ or <1% of the in-cabin $PM_{2.5}$ contributed from the tailpipe.

Hill et al. (2005) reported SP from 9 different school buses tested in three US cities using a progressive retrofit method and an LV to represent on-road background; an alternative approach to quantify tailpipe exhaust and crankcase emissions. However, these results did not permit reliable quantification of SP as these measurements were not exclusive to the specific bus sources. Borak and Sirianni (2007) reviewed 11 different studies that measured diesel exhaust particles in school bus cabins and observed inconsistent findings across studies because of few number of tested buses, inadequate control for potential confounding, exploratory in nature and in general, due to methodological limitations.

Our study aimed to quantify the levels and major sources of a bus's SP using dual tracers (DT) and two other independent methods. We used the fuel-based Ir tracer and a lube-oil-based tracer (Zielinska et al., 2008) to distinguish the tailpipe exhaust and the crankcase emissions, respectively. We adapted an on-road dilution tunnel (Weaver and Petty, 2004) to quantify the mass ratios of PM and the tracers in the emissions. We used results from the DT method as the reference to assessment the performance of the LV and chemical mass balance (CMB) methods.

Methods

This study was conducted during summer 2005 on 2 Seattle school buses. Bus 1 was a 2003 model (49,012 miles), the median model year of Seattle school buses, equipped with a

manufacturer-installed diesel oxidation catalyst (DOC). Bus 2, a year 2000 model (79,482 miles), was retrofit with an AZ Purimuffler/Purifier DOC (Engine Control System). The study was conducted in two phases, in the first phase in cabin measurements were made and in the second, source sampling was done. A schematic of bus and LV measurements are shown in Figure 1. The first phase of this study involved two days of four in-cabin runs per bus; 2 runs with windows closed or open, respectively. During each run the bus drove back and forth along a residential route with little truck traffic. Each run consisted of 27 stops with 1-min idling. A 1996 Chrysler Minivan with a new engine served as the LV and drove ~5 min ahead of the bus with its fan off and windows open to monitor on-road background levels. Marine batteries and inverters powered the equipment on the bus and LV. After the in-cabin monitoring, all instruments were removed from the bus for the second phase, source monitoring.

Tracers

Tris(norbornadiene)iridium(III)acetylacetonate, an organometallic iridium complex, was dissolved in toluene (1g:225 ml) and added to each bus' fuel tank to track tailpipe exhaust particulate. Fully deuterated normal hexatriacontane (n-$C_{36}D_{74}$ or d-alkane) was dissolved in the bus' lubricant oil (100g:18.9L) to track crankcase emissions. The lubricant oil from Bus 1 was transferred after testing to Bus 2. Fuel-based Ir tracer was selected as it has been shown to be representative, highly specific and sensitive to exhaust emissions. For the lubricating oil, d-Heaxatricontane (n-$C_{36}D_{74}$) was chosen as crankcase emissions were assumed to consist primarily of the higher molecular weight hydrocarbons in oil that were either aerosolized by blow-by past the piston rings or were vaporized and condensed onto fine particles. n$C_{36}H_{74}$ occurs naturally among high molecular weight compounds of lubricating oil, hence could be estimated with high sensitivity and specificity using GC-MS methods.

In-cabin and LV Sampling

Integrated $PM_{2.5}$ samples were collected on 47-mm Teflon and quartz filters using 4 UMD samplers (University of Maryland) at 120 L/min. The UMD samplers consisted of a 6″ glass inlet with an impaction section and an o-ring flange joint attached to another 6″ glass and a filterpack. The impactor is designed to achieve a particle size cutpoint of 2–3 mm at 120 L/min (Lin, December 1993). Two UMD samplers (with a Teflon and a quartz filters, respectively) were exposed for the entire bus run (2.4±0.5 h), while two other samplers (one Teflon and one quartz filters) were exposed for each half of the runs (forward vs. reverse, 1.2±0.3 h). Two BGI samplers (BGI Inc., Waltham, MA) with 1-μm sharp-cut cyclone (Kenny et al., 2000) and 47-mm Teflon filters at 16.7 L/min were exposed for the entire run.

PM was monitored continuously with various monitors; some used in previous studies as markers for specific bus emission sources. The active pDR (retrofitted 1000AN, Thermo Electron Corp., Franklin, MA) with a 2.5-μm sharp-cut cyclone at 4 L/min measured light scattering (Chakrabarti et al., 2004). The pDR was factory-calibrated with the fine ISO test dust (specific gravity 2.6, refraction index =1.5 – 0i, d_p50=2–3 μm) and was zeroed before each sampling period (Liu et al., 2003; Liu et al., 2002). The P-TRAK (Model 8525, TSI, Inc., Shoreview, MN), which is a condensation particle counter, measured number concentrations of particles with aerodynamic diameters between 0.02 and 1 μm. An Aethalometer with a 2.5-μm sharp-cut cyclone at 5 L/min was used to monitor BC using the 880-nm channel (Model AE-42, Magee Scientific, Inc., Berkeley, CA). Aethalometers measure BC by determining the attenuation of the light transmitted through a sampled filter (Hansen et al., 1984). BC was also monitored with a photoacoustic monitor using a power-modulated laser light at 1047 nm at operation frequency of an acoustical resonator (Arnott et al., 2005). The photoacoustic monitor was calibrated prior to and after field monitoring by

measuring the absorption of a known concentration of NO_2. We also used the photoelectric aerosol sensor (PAS 2000CE, EcoChem Analytics, League City, TX) to measure polycyclic aromatic hydrocarbons (PAHs). The PAS utilizes UV radiation (222 nm) produced by a KrBr excimer lamp to ionize surface-bound PAHs on PM_1 (Burtscher, 1992; Tang et al., 2000; Wallace, 2005). All continuous instruments were cushioned to reduce vibration. Duplicate P-TRAK and PAS were deployed. All the monitors and sampling devices were located in the middle of the bus. The LV was equipped with identical instrumentation, with gravimetric samples integrated over the entire run.

Source Sampling

During the second phase, each bus was driven along portions of the same route for three 30-min runs of tailpipe sampling and three 15 to 30-min runs of crankcase sampling. Source sampling was conducted after the first phase in-cabin sampling to avoid any possibility of bus interior contamination with either tracers. The “Ride Along Vehicle Emission Measurement” system (RAVEM) (Weaver and Petty, 2004; Zielinska et al., 2008) was used to collect PM samples and monitor engine performance. The RAVEM is based on proportional partial-flow constant volume sampling, whereby exhaust or crankcase blow-by entering the system at a variable rate is pumped out of the system at a constant rate. Isokinetic tailpipe sampling followed by dilution resulted in a diluted exhaust stream which was collected by University Research Glass (URG) samplers with sharp $PM_{2.5}$ Cyclone inlet (URG, Chapel Hill, NC) at a flow rate of 16.7 L/min. For each test run, a Teflon and a quartz sample were collected from the dilution tunnel and in addition a third sample (alternating Teflon and quartz) was collected upstream of emission injection point to serve as a field blank. The RAVEM provided additional 4th port in the manifold for sampling PM_1 using a BGI sampler with Teflon filter (at 16.7 L/min). For crankcase vent emission sampling, the RAVEM dilution tunnel was mounted on the front bumper of each bus and full flow from the crankcase vent was directly ducted into the tunnel. Similar to tailpipe sampling, three $PM_{2.5}$ and one PM_1 samples were collected for each crankcase test runs.

Sample Handling and Chemical Analysis

All in-cabin samples were stored separately and analyzed several weeks before the source samples to avoid cross-contamination. All Teflon filters were weighed with a 7-place electronic UMT2 ultramicrobalance (Mettler Toledo, Greifensee, Switzerland). PM_1 filters were analyzed for trace elements with X-ray fluorescence. $PM_{2.5}$ Teflon filters were analyzed for Ir by instrumental neutron activation analysis (Suarez et al., 1998) and not subject to XRF to avoid potential losses of Ir. Quartz filters were analyzed for organics including d-alkane (Zielinska et al., 2008). Organic carbon and elemental carbon were analyzed using the Thermal-Optical Reflectance (TOR) method following the Interagency Monitoring of Protected Visual Environments protocol. The remainder of each quartz filter was extracted with dichloromethane/hexane using accelerated solvent extraction (Dionex 300) and analyzed for PAHs, hopanes/steranes and alkanes by GC/MS (Zielinska et al., 2008).

Data Analysis

We used the DT method to estimate SP attributable to the diesel exhaust particles from the tailpipe (PM_{tp}) and $PM_{2.5}$ from the crankcase emissions (PM_{ck}):

$$SP = PM_{tp} + PM_{ck} = Ir_{bus} * (PM_{tp}/Ir_{tp}) + d-alkane_{bus} * (PM_{ck}/d-alkane_{ck}) \quad (1)$$

where the ratios of PM_{tp} and Ir in tailpipe exhaust (Ir_{tp}) and PM_{ck} to d-alkane in crankcase exhaust (d-$alkane_{ck}$) were obtained from the source samples. Ir in crankcase and d-alkane in

tailpipe were negligible. The PM_{ck}/d-alkane$_{ck}$ ratio was computed by dividing the estimated total carbon mass by the d-alkane mass. Ratios were averaged across the three crankcase or three tailpipe runs for each bus.

The LV method estimates SP as the difference in pollutant concentrations between the bus and LV. The two-sample t-test was used for continuous measurements to examine differences in concentrations between bus and LV and differences in SP levels between windows configurations. Both t-test and Wilcoxon rank sum test were used for integrated samples due to the small sample size.

The CMB method (CMB-8.2) (U.S. EPA, 2004; Watson et al., 2001) consists of linear equations in which concentrations of individual chemical species are expressed as linear sums of products of the mass fraction of the species in particle emissions from each source (i.e., tailpipe, crankcase, and 'other') and source contributions. Solutions were achieved using weighted least-squares fit. Our main inputs were the $PM_{2.5}$ organic species, PM_1 trace elements, mass fractions of individual species in the source profiles, and the uncertainties of individual species (U.S. EPA, 2004; Watson et al., 2001). As the conventional CMB method had difficulties resolving profiles with many highly correlated organic species, we used the partial least squares (PLS) regression to identify major species for individual source profiles to include in the conventional CMB.

Quality Control

The percentage of the number of valid samples among all deployed samples, was 85%, 95%, and 95% for the LV, bus, and source samples, respectively. Most missing or voided samples were due to pump failures or broken filters. All reported concentrations were blank corrected. Monitor precision and limit of detection are reported in Supplement Table S1. Precision for the UMD sampler was based on the difference between the 2-h samples and the average of the collocated half-run samples. The relatively low precision for the UMD sampler was due to leakage and variable flow rates of the 2-h sample pump in two runs. For $PM_{2.5}$ mass concentrations, the average of the two half-run UMD samples were thus used for analysis. For Ir and organic species, the volume weighted averages of the concurrent samples were used. The sensitivity of the Ir tracer method was 0.002 $\mu g/m^3$ for diesel particulate matter (Ireson et al., 2004), while the LOD for d-alkane was 0.03 $\mu g/m^3$ (Zielinska et al., 2008).

Results

In-Cabin Measurements

PM_1 and $PM_{2.5}$ concentrations averaged 10 and 22 $\mu g/m^3$, respectively (Table 1). On average, PM_1 was 43±17% of the $PM_{2.5}$ mass. The pDR readings overestimated the gravimetric $PM_{2.5}$ measurements but correlated very well with the PM_1 measurements, with an R^2 of 0.99 for the on-bus measurements (supplement Figure S1a). Most continuous monitors, except for P-TRAK, measured higher concentrations on Bus 2. The closed-windows configuration saw higher levels of PM_1, $PM_{2.5}$, OC, EC, and PAHs. The PAH readings from the PAS correlated with those from the GC/MS method (R^2=0.70, PAH (ng/m^3)=−2.6+0.08*PAS). The on-bus Aethalometer and photoacoustic measurements correlated with EC from the TOR method (R^2=0.83–0.86) (Figure S1b).

Lead Vehicle Measurements

PM_1 and $PM_{2.5}$ concentrations in the LV averaged 5 and 19 $\mu g/m^3$, respectively (Table 2). $PM_{2.5}$ was significantly higher than the corresponding background $PM_{2.5}$ concentration at a regional background site. PM_1 was 25±18% of the $PM_{2.5}$ mass inside the LV, indicating

more coarse particles in the on-road background than on the bus. As levels of most PM constituents were lower in the LV, more uncertainties were involved in continuous measurements (Figure S1). Nevertheless, the overall R^2 between pDR and PM_1 still reached 0.86 (PM_1=3.2+0.2*pDR).

Self Pollution Estimates from the Dual Tracers Method

Results from source samples indicated that the mass ratio of $PM_{2.5}$ to tracers was similar across runs within each bus. The ratios of Ir/d-alkane in the tailpipe samples were at least 1000 times those in the crankcase samples, indicating sensitive tracers for separating these two sources. Our estimated in-cabin PM_{tp} and PM_{ck} averaged 1.1 μg/m^3 and 6.8 μg/m^3, respectively (Table S2). On average, PM_{ck} was 77% of the SP, which accounted for one-third of the in-cabin $PM_{2.5}$. PM_{tp} accounted for 5% and 9% of the in-cabin $PM_{2.5}$ and PM_1, respectively. Pollution from sources other than SP contributed an average of 16 μg/m^3 (or 66%) to the in-cabin $PM_{2.5}$. SP was not significantly different between buses. Using 1-h measurements (more samples) for comparisons between buses and window configurations, we verified higher PM_{tp} aboard the older Bus 2 and higher levels of PM_{tp} and PM_{ck} with windows closed (Table S2). With closed windows, SP averaged 13 μg/m^3 or 46% of the in-cabin $PM_{2.5}$.

Self Pollution Estimates from the Lead Vehicle Method

The LV-SP estimates from various monitors were mostly positive except for the PAS (Table 3). SP averaged 3 μg/m^3 for PM_1, 1.7 and 7.1 μg/m^3 for EC and OC, respectively from the TOR method, and 18,300 counts/cm^3 of ultrafine particles. The LV-SP estimates for PM_1, $PM_{2.5}$, BC, EC, and OC were higher with closed windows. Negative LV-SP estimates indicated higher background pollution levels than those in the cabin, due partially to instrumental uncertainties at low SP pollution levels and different traffic conditions encountered by the bus and LV. Negative LV-SP estimates from $PM_{2.5}$ measurements could also result from the 50% size-cut efficiency of the UMD sampler as well as resuspended road dust encountered by the lower monitoring platform in the LV than on the bus. Thus, $PM_{2.5}$ measurements may not provide the best indicator for SP. For the PAS and the photoacoustic measurements, the differences between the bus and the LV were close to the instrumental noise.

Table 4 provides correlations between the LV-SP and tracer estimates. SP estimates from EC, PAHs (GC/MS), and PM_1 measurements had the highest correlations with PM_{tp} (Figure 2a–d). EC-TOR explained 96% of the variability in tracer PM_{tp} estimates. Most LV-SP overestimated PM_{tp}, except for PAS and the photoacoustic monitor. LV-SP estimates using the OC-TOR and pDR measurements explained 87% and 89% of the variability in tracer PM_{ck} estimates, respectively (Figure 2e,f). Excluding one sample with an OC_4 outlier (28 μg/m^3) in the forward run 3 of Bus 1, which was much higher than others (<2.8 μg/m^3), the R^2 for OC-TOR and PM_{ck} became 0.95 (OC = 0.94 * PM_{ck} regression without intercept). SP estimates from continuous EC measurements did not significantly correlate with PM_{ck}, indicating EC as a potential marker for PM_{tp}. SP estimates from P-TRAK did not correlate with estimates from other monitors (Table 4).

Available 1-h SP estimates from the DT and LV methods were added to verify results from the 2-h measurements (Figure 3). Both Aethalometer and photoacoustic provided good indicators for PM_{tp} (Figure 3a–b). All continuous LV-SP estimates, however, reached a plateau at higher PM_{tp} values. The correlation between the LV-SP estimates from the calibrated pDR measurements and PM_{ck} remained high using 1-h measurements (R^2=0.80, Figure 3g).

Self Pollution Estimates from the CMB Method

Table S3 shows summary profile of trace elements and detailed organic species from the bus, LV, and source samples. For tailpipe emissions, EC and OC were 73±46% and 25±6% of the emitted $PM_{2.5}$ mass, respectively. For crankcase emissions, EC and OC were 2±1% and 74±23% of the emitted $PM_{2.5}$ mass, respectively. The PLS analysis identified sulfur, EC1, EC2, EC, 2 alkanes, 4 hopanes, and 3 steranes as important species to include in CMB. The CMB model estimated an average contribution of 1.9, 9.9, and 3.5 $\mu g/m^3$ from tailpipe, crankcase, and other sources, respectively (Table S2). Crankcase emissions contributed an average 78±10% of $PM_{2.5}$ to SP. These results overestimated but correlated well with those from the DT method (Figure 4), with a Pearson correlation coefficient of 0.98 for CMB_{ck} and PM_{ck} and 0.86 for CMB_{tp} and tracer PM_{tp} (Table 4). Contributions from other sources to the in-cabin pollution, estimated by CMB-PLS based on the LV profile, were generally smaller than the total CMB-SP and the difference between the in-cabin $PM_{2.5}$ and DT-SP (blue crossed-shadow bars in Figure 3).

Discussion

Both DT and CMB methods quantified the crankcase emissions as the primary SP source in our study buses. These PM_{tp} estimates were higher than those reported by Ireson et al. (2004) and Wu et al. (1998) but significantly lower than those by Behrentz et al. (2004), which could be partially due to the differences in bus models, driving conditions, fuel used, retrofit technologies used, and the methodology. Borak and Sirianni (2007) reviewed 11 studies of SP in 58 diesel school buses and highlighted the differences in methodologies resulting in the disagreement in their findings. We used the combination of fuel- and lube-oil-based tracers, while previous studies employed only one tracer for tailpipe exhaust. Previous studies used either a chassis dynamometer off-road (Ireson et al., 2004) or did not measure the PM:tracer ratios directly in the tailpipe exhaust (Behrentz et al., 2004; Wu et al., 1998). We established the actual PM:tracer ratios in emissions through source testing on the same bus route as during the in-cabin sampling runs. Furthermore, the DT method was validated with its close agreement with those from the CMB-PLS without utilizing tracers.

All EC and gravimetric PM_1 measurements from the LV method correlated well with the PM_{tp} from the DT method. The OC-TOR and pDR measurements provided adequate estimates for PM_{ck}. However, measurements of EC/OC-TOR and gravimetric PM_1 require high-volume pumps to overcome the detection limit constraint for the short sampling duration. These aforementioned measures thus are not feasible for regular field monitoring, with the exception of mobile Aethalometers and photoacoustic monitors. The LV method using the active pDR, which involves only a small battery-powered personal pump, provided a feasible and affordable means for relative quantification of PM_{ck}. The LV-pDR method needs to be calibrated against a reference method (e.g., the tracer method) to accurately reflect PM_{ck} levels. Further studies are needed to confirm a consistent relationship between EC measurements and PM_{tp} and between pDR and PM_{ck} across buses with varying environmental and traffic conditions.

Although Hill et al. (2005) used P-TRAK for monitoring tailpipe exhaust, the SP estimates from our LV-P-TRAK method showed no associations with the tracer-based PM_{tp} and other SP estimates. Nor did we observe any dependence of particle counts on window configuration. P-TRAK often spiked in spite of no detectable pollution events. SP estimates from the PAS monitor were mostly negative but still correlated with the SP estimates from PM_1 and PAHs (GC/MS). With relatively constant PAH levels in LV, this indicated proportional but noisy SP estimates from the PAS at low SP levels. Further evaluation of these two instruments is needed for SP assessment.

The CMB method with the PLS selection of source profiles provided separate contribution estimates for tailpipe, crankcase, and other sources. The CMB estimates for PM_{tp} were similar to those of the LV-SP from EC and correlated with those from PAHs (GC/MS). CMB estimates for PM_{ck} showed better agreement with tracer-PM_{ck} than any LV-SP estimates. Both CMB and LV-SP for most PM constituents overestimated tracer PM_{tp}. We could not completely rule out the possibility of underestimation by the Ir tracer method. Future studies that measure PM emission rates with and without the Ir tracer would verify the accuracy of the Ir tracer estimates for PM_{tp}. The CMB method underestimated contributions from other sources, as compared with those from the LV method or the urban background levels. It is possible that there are bus emission sources other than the tailpipe and crankcase, e.g., brake and tire wear, that are not identified by our DT method or source profiles used by the CMB. However, this underestimation is also likely due to the greater uncertainties associated with the LV profile at low concentrations.

One major strength of this study is the use of 3 independent methods to quantify the bus' self pollution and to shed light on future applications of these various methods in exposure assessment or epidemiological studies. One other strength is our capability to characterize the in-cabin air pollution originated from "other" sources, namely the exhaust from other on-road vehicles using the LV and CMB methods. In our study, measurements in the LV provided concurrent concentrations from other on-road and background sources. Some uncertainties were particular to our study design in that the LV was driven 5 minutes ahead of the bus to prevent tracer contamination from the bus emissions. For average roadway $PM_{2.5}$ exposures, this may provide a reasonable estimate. However, we recognize that for short-term spikes in particle number, Black Carbon concentrations the immediate vicinity of the measuring vehicle could be more important and hence the present method may not estimate general roadway exposure levels for these pollutants. Thus, in studies using LV without tracers, the LV could be driven as closely as possible ahead of the bus as long as it is upwind or not influenced by the bus exhaust.

Buses with open windows allow for higher infiltration efficiency of outdoor air and thus increased dilution of SP if outdoor air was cleaner. Previous research has shown similar effects of window configuration (Behrentz et al., 2005; Marshall and Behrentz, 2005; Sabin et al., 2005a; Sabin et al., 2005b; Solomon et al., 2001; Wargo, 2002). In more polluted cities, the outdoor air could have higher $PM_{2.5}$ than in-cabin air and thus opening windows might not reduce total in-cabin pollution as observed in our study. We conducted this study specifically in a residential area without much truck traffic such that effects of SP are unambiguous from other sources.

Earlier studies have shown the effect of meteorological factors e.g wind from the front to the back of the bus or wind speed (strong winds vs calm breeze) on bus in cabin pollutant levels (Adar et al., 2008; Borak and Sirianni, 2007; Hill et al., 2005). Thus that could lead to additional uncertainty in our SP estimates and may not be generalized to different weather conditions. We recognize that this study tested only two buses representative of the characteristics of the bus fleet in the Seattle School District as of 2005. Both buses were equipped with the DOC and ran on ultra-low sulfur diesel fuel. For more accurate and representative assessment of the buses' SP and the effectiveness of any retrofit programs, it will be important to examine buses of various ages, with and without DOC, with and without crankcase ventilation, and with or without a diesel particle filter.

Supplementary Material

Refer to Web version on PubMed Central for supplementary material.

Acknowledgments

This study was partially sponsored by the National Institute of Environmental Health Sciences, a gift fund from the International Truck and Engine Corporation with the University of Washington, and the U.S. Department of Energy Office of FreedomCAR and Vehicle Technologies through the National Renewable Energy Laboratory. We thank the technical supports from David Anderson of the Seattle School District Transportation Department, First Student, Inc., the Puget Sound Clean Air Agency, and Bruce Hill of Clean Air task Force.

List of acronyms

SP	self pollution
DT	dual tracer
LV	lead vehicle
RAVEM	ride along vehicle emissions measurement system
PMck	crankcase PM
PMtp	tailpipe PM
UMD	University of Maryland
PLS	partial least square
PAH	polycyclic aromatic hydrocarbons
DOC	diesel oxidation catalyst
PAS	photoelectric aerosol sensor
pDR	personal DataRAM
TOR	thermal optical reflectance
CMB	chemical mass balance

References

Adar SD, Davey M, Sullivan JR, Compher M, Szpiro A, Liu LJS. Predicting airborne particle levels aboard Washington State school buses. Atmospheric Environment 2008;42(33):7590–7599. [PubMed: 18985175]

Arnott W, Zielinska B, Rogers C, Sagebiel J, Park K, Chow J, et al. Evaluation of 1047-nm photoacoustic instruments and photoelectric aerosol sensors in source-sampling of black carbon aerosol and particle-bound PAHs from gasoline and diesel powered vehicles. Environmental Science and Technology 2005;(39):5398–5406. [PubMed: 16082972]

Behrentz E, Fitz DR, Pankratz DV, Sabin LD, Colome SD, Fruin SA, Winer AM. Measuring self-pollution in school buses using a tracer gas technique. Atmospheric Environment 2004;(38):3735–3746.

Behrentz E, Sabin LD, Winer AM, Fitz DR, Pankratz DV, Colome SD, Fruin SA. Relative importance of school bus-related microenvironments to children's pollutant exposure. Journal of the Air and Waste Management Association 2005;55(10):1418–30. [PubMed: 16295266]

Borak J, Sirianni G. Studies of self-pollution in diesel school buses: Methodological issues. Journal of Occupational and Environmental Hygiene 2007;4(9):660–668. [PubMed: 17616893]

Burtscher H. Measurement and characteristics of combustion aerosols with special consideration of photoelectric charging and charging by flame ions. Journal of Aerosol Science 1992;23:549–595.

Chakrabarti B, Fine PM, Delfino R, Sioutas C. Performance evaluation of the active-flow personal DataRAM PM2.5 mass monitor designed for continuous personal exposure measurements. Atmospheric Environment 2004;38:3329–3340.

Hansen A, Rosen H, Novakov T. The aethalometer—an instrument for the real-time measurement of optical absorption by aerosol particles. Science of the Total Environment 1984;36:191–196.

Hill LB, Zimmerman NJ, Gooch J. Investigation of the Effectiveness of Retrofit Emissions Controls in Reducing Exposures to Particulate Matter in School Buses. Clear Air Task Force report. 2005

Ireson R, Easter M, Lakin M, Ondov J, Clark N, Wright D. Estimation of diesel particulate matter concentrations in a school bus using a fuel-based tracer—a sensitive and specific method for quantifying vehicle contributions. Transportation Research Record 2004;(1880):21–28.

Kenny LC, Gussman R, Meyer M. Development of a Sharp-Cut Cyclone for Ambient Aerosol Monitoring Applications. Journal of Aerosol Science and Technology 2000;32(4):338–358.

Lin, ZC. PhD Thesis. University of Maryland; College Park, MD, USA: Dec. 1993 Development of Enriched Rare Earth Isotope Tracers for Application to Source Apportionment.

Liu LJS, Box M, Kalman D, Kaufman J, Koenig J, Larson T, Lumley T, Sheppard L, Wallace L. Exposure Assessment of Particulate Matter for Susceptible Populations in Seattle, WA. Environmental Health Perspectives 2003;111(7):909–918. [PubMed: 12782491]

Liu L-JS, Slaughter C, Larson T. Comparison of light scattering devices and impactors for particulate measurements in indoor, outdoor, and personal environments. Environmental Science and Technology 2002;(36):2977–2986. [PubMed: 12144275]

Marshall J, Behrentz E. Vehicle self-pollution intake fraction: Children's exposure to school bus emissions. Environmental Science and Technology 2005;(39):2559–2563. [PubMed: 15884349]

Rim D, Siegel J, Spinhirne J, Webb A, McDonald-Buller E. Characteristics of cabin air quality in school buses in Central Texas. Atmospheric Environment 2008;42(26):6453–6464.

Sabin LD, Behrentz E, Winer AM, Jeong S, Fitz DR, Pankratz DV, Colome SD, Fruin SA. Characterizing the range of children's air pollutant exposure during school bus commutes. Journal of Exposure Analysis and Environmental Epidemiology 2005a;15(5):377–87. [PubMed: 15592444]

Sabin LD, Kozawa K, Behrentz E, Winer AM, Fitz DR, Pankratz DV, Colome SD, Fruin SA. Analysis of real-time variables affecting children's exposure to diesel-related pollutants during school bus commutes in Los Angeles. Atmospheric Environment 2005b;(39):5243–5254.

Solomon, G.; Campbell, T.; Feuer, G.; Masters, J.; Samkian, A.; Paul, K. Natural Resources Defense Council and Coalition for Clean Air. NRDC Publications Department; 40 West 20th Street, New York, NY 10011: 2001. No Breathing in the Aisles.

Suarez AE, Caffrey PF, Borgoul PV, Ondov JM, Divita JF. Use of an Iridium Tracer to Determine the Size Distribution of Aerosol Emitted from a Fleet of Diesel Sanitation Trucks. Environmental Science and Technology 1998;32:1522–1529.

Tang, S.; Johnson, R.; Lanni, T.; Webster, W. Monitoring of PM-Bound Polycyclic Aromatic Hydrocarbons from Diesel Vehicles by Photoelectric Aerosol Sensor (PAS). Society of Automotive Engineers; 2000. Document Number: 2001-01-3578

U.S. EPA. What you should know about diesel exhaust and school bus idling. 2003. http://www.epa.gov/otaq/retrofit/documents/f03005.pdf

U.S. EPA. EPA-CMB8.2 Users Manual. Publication No. EPA-452/R-04 011. Research Triangle Park, NC: Office of Air Quality Planning & Standards; 2004.

Wallace L. Real-time measurements of black carbon indoors and outdoors: A comparison of the photoelectric aerosol sensor and the aethalometer. Aerosol Science and Technology 2005;39(10): 1015–1025.

Wargo, J. Children's exposure to diesel exhaust on school buses. Environmental and Human Health, Inc; North Haven, CT: 2002.

Watson J, Chow J, Fujita E. Review of Volatile Organic Compound source apportionment by chemical mass balance. Atmospheric Environment 2001;35:1567–1584.

Weaver, C.; Petty, L. Reproducibility and accuracy of on-board emissions measurements using the RAVEM system. SAE International; 2004. Paper No. 2004-01-0965

Wu CC, Suarez AE, Lin Z, Kidwell CB, Borgoul PV, Caffrey PF, Ondov JM, Sattler B. Application of an Ir tracer to determine soot exposure to students commuting to school on Baltimore public buses. Atmospheric Environment 1998;(32):1911–1919.

Zielinska B, Campbell D, Lawson DR, Ireson RG, Weaver CS, Hesterberg TW, Larson T, Davey M, Liu LJS. Detailed characterization and profiles of crankcase and diesel particulate matter exhaust

emissions using speciated organics. Environmental Science and Technology 2008;42(15):5661–5666. [PubMed: 18754490]

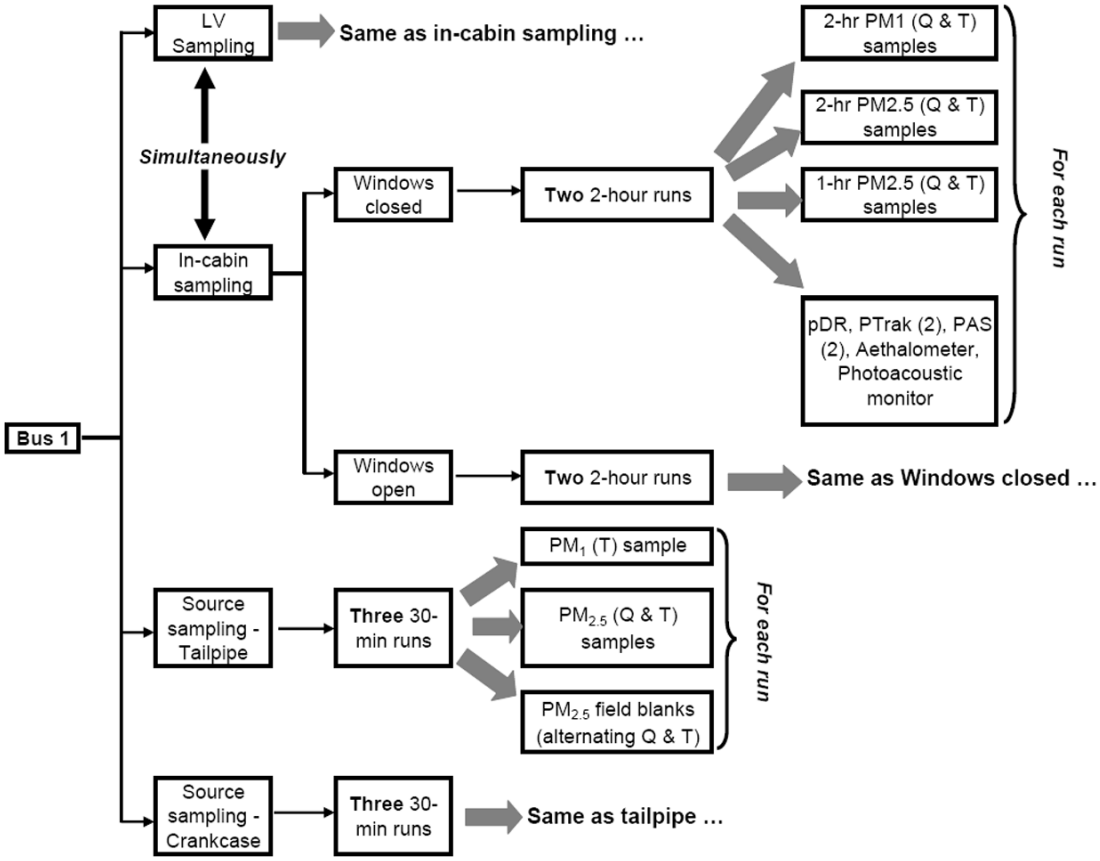

Figure 1.
Schematic of various measurements made in bus cabin, on LV and during tailpipe and crankcase sampling.

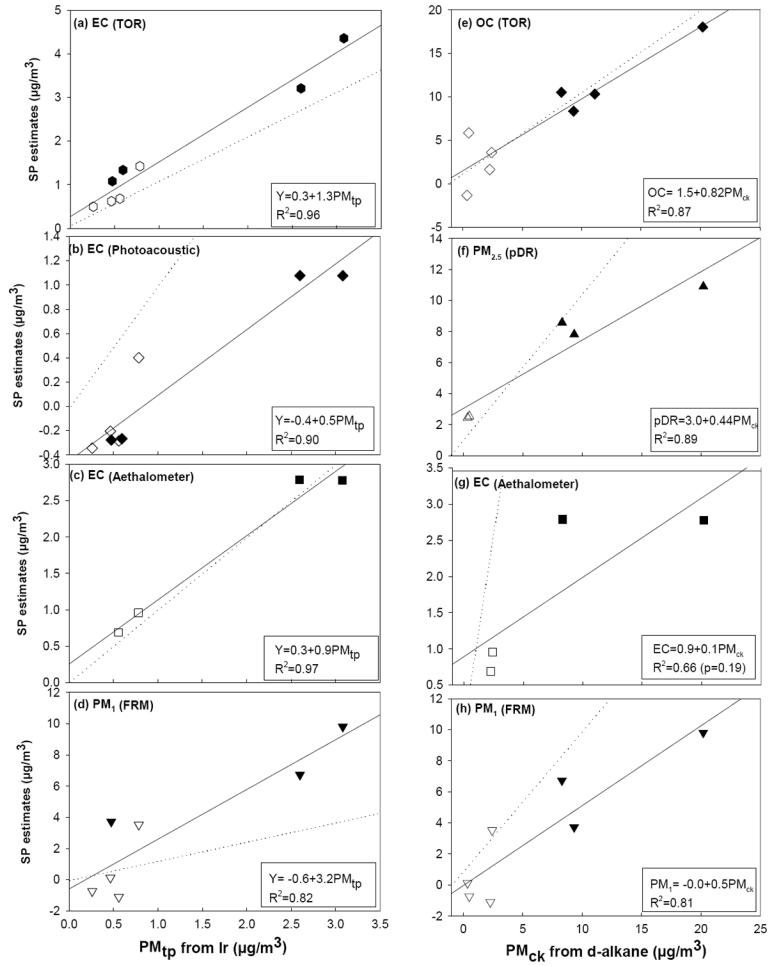

Figure 2.

Comparison of 2-h self-pollution estimates from the LV method with different measurements vs. the tracers estimates for PM from the tailpipe (PM_{tp}) and crankcase (PM_{ck}). Filled and void symbols represent window open and closed runs, respectively. A 1:1 dotted line is also included for reference.

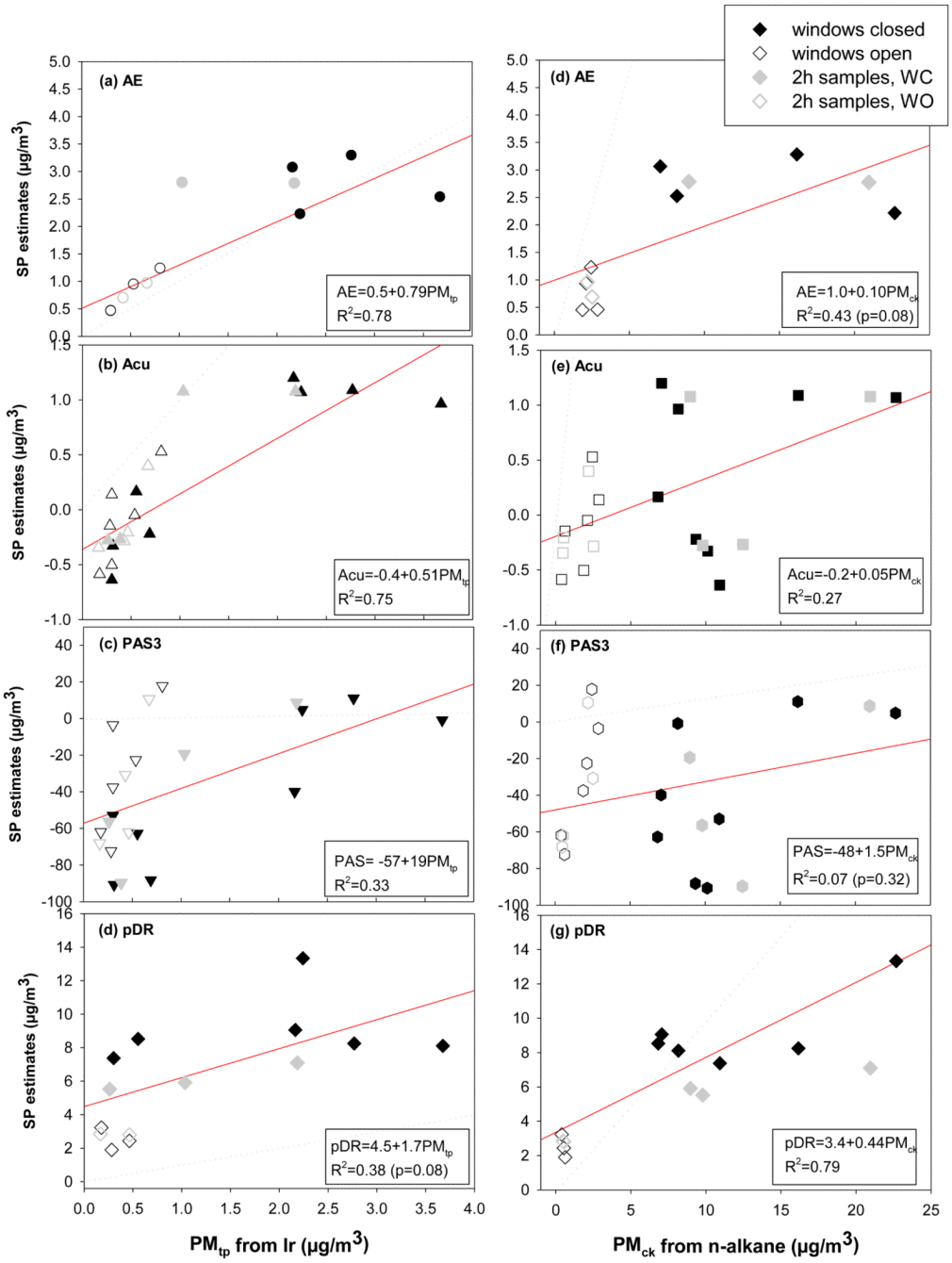

Figure 3.
One-hour self-pollution estimates (red symbols) from the LV method vs. the tracer estimates for tailpipe (PM_{tp}) and crankcase $PM_{2.5}$ (PM_{ck}). The 2-h samples and a 1:1 dotted line are included for reference.

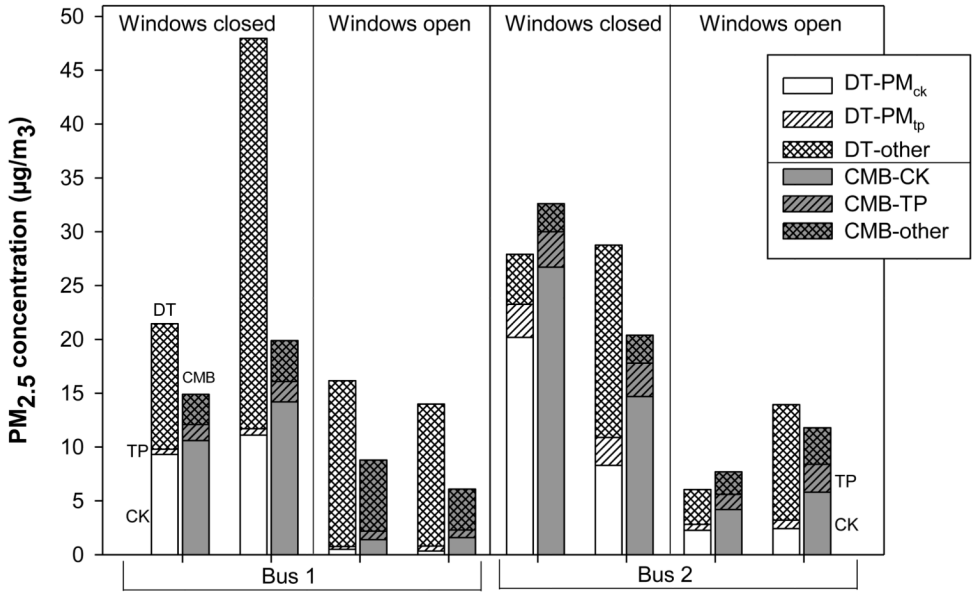

Figure 4.

Estimates of in-cabin $PM_{2.5}$ contributions from the tailpipe (TP), crankcase (CK), and other sources using the dual tracers (DT) and the chemical mass balance (CMB) with partial least square methods.

Table 1

Summary of on-bus measurements of integrated gravimetric and continuous data. N represents the number of integrated samples or 1-min measurements. Differences between buses 1 and 2 or window configurations are shown in the last column.

Measure	Bus	Window	N	Mean	Std	Min	Max	Difference (range)
PM_1 (μg/m^3)	1		8	11	5	7	19	3 (−2,8)
	2		8	8	5	3	14	
	Both	C	8	14	3	10	19	8 (5,11)‡
		O	8	5	2	3	8	
	Both		16	10	5	3	19	
$PM_{2.5}$ (μg/m^3) from UMD	1		8	25	16	14	61	6 (−9,20)
	2		8	19	11	3	34	
	Both	C	8	32	13	19	61	19 (8,29)≠
		O	8	13	5	3	18	
	Both		16	22	14	3	61	
pDR (μg/m^3)	1		511	34	31	6	210	−24 (−29, −19)≠
	2		288	58	41	6	224	
	Both	C	473	58	40	6	224	37 (32,42)‡
		O	326	20	14	6	203	
	Both		799	43	37	6	224	
UPM (#/cm^3) from P-TRAK (PT)	1		341	44587	43153	5611	169948	19387 (15118,23657)‡
	2		497	25200	18340	2069	158783	
	Both	C	460	26336	22013	5611	159366	−14970 (−19262, −10678)≠
		O	378	41306	40128	2069	169948	
	Both		838	33089	32351	2069	169948	
PAH (ng/m^3) from GC/MS	1		4	1.1	0.5	0.6	1.7	−1.1 (−2.6,0.5)
	2		4	2.1	1.2	1.0	3.3	

Measure	Bus	Window	N	Mean	Std	Min	Max	Difference (range)
	Both	C	4	2.3	1.0	1.2	3.3	1.4 (0.1,2.6)†
		O	4	0.9	0.3	0.6	1.3	
	Both		8	1.6	1.0	0.6	3.3	
PAH (ng/m^3) from PAS	1		659	44	39	0	193	−18 (−23, −13)‡
	2		504	61	47	0	440	
	Both	C	615	54	42	0	259	6 (1,11)†
		O	548	48	45	0	440	
	Both		1163	51	43	0	440	
EC (μg/m^3) from aethalometer	1		602	1.1	0.8	−0.2	8.8	−1.7 (−1.8, −1.5)‡
	2		478	2.8	2.1	−0.1	15.1	
	Both	C	583	2.5	1.8	−0.2	7.6	1.3 (1.1,1.5)‡
		O	497	1.1	1.4	−0.1	15.1	
	Both		1080	1.9	1.7	−0.2	15.1	
EC (μg/m^3) from photoacoustic	1		618	0.5	0.5	−0.1	7.2	−0.9 (−0.9, −0.8)‡
	2		504	1.3	1.0	−0.1	8.1	
	Both	C	574	1.2	0.9	−0.1	3.3	0.7 (0.6,0.8)‡
		O	548	0.5	0.7	−0.1	8.1	
	Both		1122	0.9	0.9	−0.1	8.1	
EC (μg/m^3) from TOR	1		4	1.9	0.6	1.3	2.7	−1.5 (−3.6,0.5)
	2		4	3.5	1.5	1.8	5.2	
	Both	C	4	3.6	1.4	2.1	5.2	1.3 (−0.1,3.6)
		O	4	1.8	0.6	1.3	2.7	
	Both		8	2.7	1.4	1.3	5.2	
OC (μg/m^3) from TOR	1		4	13.9	5.7	6.6	20.6	−1.9 (−11.4,11.3)

Measure	Bus	Window	N	Mean	Std	Min	Max	Difference (range)
	2		4	13.9	7.3	6.5	23.1	
	Both	C	4	18.6	3.9	14.6	23.1	9.4 (3.0,15.8)†
		O	4	9.2	3.5	6.5	13.9	
	Both		8	13.9	6.1	6.5	23.1	

† p<0.05,

≠ p<0.01,

‡ p<0.001

Table 2

Summary of the lead-vehicle measurements for integrated gravimetric PM_1 and $PM_{2.5}$ and continuous (1-min) data.

Measure	Bus	N	mean	std	min	max
PM_1 (μg/m^3)	1	3	8	1	7	8
	2	4	3	3	−1	6
	both	7	5	3	−1	8
$PM_{2.5}$ (μg/m^3)	1	3	26	9	18	36
	2	4	13	5	6	18
	both	7	19	10	6	36
pDR (μg/m^3)	1	425	26	13	0	78
	2	287	17	14	0	95
	both	712	22	14	0	95
UPM (#/cm^3) from PT	1	427	14631	9462	4240	91918
	2	495	13952	11881	1902	103133
	both	922	14266	10828	1902	103133
PAH (ng/m^3) from PAS	1	569	130	122	0	550
	2	511	132	117	0	749
	both	1080	131	119	0	749
PAH (ng/m^3) from GC/MS	1	4	0.8	0.3	0.6	1.3
	2	4	0.9	0.3	0.5	1.3
	both	8	0.9	0.3	0.5	1.3
EC (μg/m^3) from Aethalometer	1[a]	48[a]	0.9	0.9	0.3	5.7
	2	496	0.9	1.0	0.0	9.5
	both	544 [a]	0.9	1.0	0.0	9.5
EC (μg/m^3) from photoacoustic	1	567	0.7	0.5	0.0	2.9
	2	446	0.7	0.6	0.0	4.5
	both	1013	0.7	0.6	0.0	4.5

Measure	Bus	N	mean	std	min	max
EC (μg/m^3) from TOR	1	4	1.1	0.3	0.7	1.4
	2	4	1.1	0.2	0.9	1.3
	both	8	1.1	0.2	0.7	1.4
OC (μg/m^3) from TOR	1	4	8.1	1.6	6.3	10.3
	2	4	5.5	0.7	4.8	6.4
	both	8	6.8	1.8	4.8	10.3
Background $PM_{2.5}$ (μg/m^3)[b]	1	4	11	2	9	12
	2	4	6	1	4	7
	both	8	8	3	4	12

[a] Malfunctioned for most Bus1 runs, which were not analyzed for self-pollution.

[b] Concurrent TEOM $PM_{2.5}$ measurements at an urban background site, Beacon Hill, Seattle.

Atmos Environ. Author manuscript; available in PMC 2011 September 1.

Table 3

Self-pollution estimates from the lead-vehicle approach, with pDR shown in calibrated values against PM_1 (i.e., pDR^c=3.17+0.16*pDR from Figure S1).

Measure	Bus	Window	N	Mean	Std	Min	Max
PM_1 (μg/m^3)	1		3	1	2	−1	4
	2		4	5	5	−1	10
	both	C	3	7	3	4	10
	both	O	4	0	2	−1	4
	both		7	3	4	−1	10
$PM_{2.5}$ (μg/m^3)	1		3	−5	8	−10	4
	2		4	6	11	−9	15
	both	C	3	10	6	4	15
	both	O	4	−5	9	−10	8
	both		7	1	11	−10	15
pDR^c (μg/m^3)	1		0	.	.	.	.
	2		4	1.8	1.1	0.7	2.8
	both	C	2	2.8	0.0	2.8	2.8
	both	O	2	0.8	0.2	0.7	1.0
	both		4	1.8	1.1	0.7	2.8
UPM (#/cm^3) from PT	1		2	31040	32061	8369	53710
	2		4	11881	3319	8342	16168
	both	C	3	10461	2053	8369	12473
	both	O	3	26073	24252	8342	53710
	both		6	18267	17609	8342	53710
PAH (ng/m^3) from PAS	1		4	−87	9	−98	−77
	2		4	−70	16	−88	−53

Measure	Bus	Window	N	Mean	Std	Min	Max
	both	C	4	−77	19	−98	−53
	both	O	4	−80	12	−90	−63
	both		8	−79	15	−98	−53
PAH (ng/m^3) from GC/MS	1		4	0.2	0.3	−0.2	0.6
	2		4	1.3	0.9	0.5	2.4
	both	C	4	1.2	0.9	0.4	2.4
	both	O	4	0.2	0.4	−0.2	0.6
	both		8	0.7	0.8	−0.2	2.4
EC (μg/m^3) from Aethalometer	1		0	.	.	.	.
	2		4	1.8	1.1	0.7	2.8
	both	C	2	2.8	0.0	2.8	2.8
	both	O	2	0.8	0.2	0.7	1.0
	both		4	1.8	1.1	0.7	2.8
EC (μg/m^3) from photoacoustic	1		4	−0.3	0.1	−0.3	−0.2
	2		4	0.6	0.7	−0.3	1.1
	both	C	4	0.4	0.8	−0.3	1.1
	both	O	4	−0.1	0.3	−0.3	0.4
	both		8	0.1	0.6	−0.3	1.1
EC (μg/m^3) from TOR	1		4	0.9	0.4	0.5	1.3
	2		4	2.4	1.7	0.7	4.4
	both	C	4	2.5	1.6	1.1	4.4
	both	O	4	0.8	0.4	0.5	1.4
	both		8	1.7	1.4	0.5	4.4

Measure	Bus	Window	N	Mean	Std	Min	Max
OC ($\mu g/m^3$) from TOR	1		4	5.8	5.1	−1.3	10.3
	2		4	8.4	7.4	1.6	18.0
	both	C	4	11.8	4.3	8.3	18.0
	both	O	4	2.4	3.0	−1.3	5.8
	both		8	7.1	6.1	−1.3	18.0

Table 4

Pearson correlation coefficients of self-pollution estimates from different measures. Yellow highlights indicate p<0.05 for both of the Pearson and Spearman (not shown) correlation coefficients. (AE=Aethalometer, Acu=photoacoustic, PT=P-TRAK)

		PMck	CMBtp	CMBck	UMD	PM1	pDRc	AE	Acu	PT	PAS	PAH	EC-TOR	OC-TOR
PMtp		**0.73**	**0.86**	**0.84**	0.71	0.90	0.83	0.99	**0.95**	−0.32	0.61	**0.96**	**0.98**	0.75
		0.039	0.006	0.010	0.076	0.005	0.083	0.013	0.000	0.538	0.105	0.000	<.0001	0.031
		8	8	8	7	7	5	4	8	6	8	8	8	8
PMck	corr	0.70	**0.98**	0.66	**0.90**	**0.95**	0.81	0.58	−0.45	0.46	**0.83**	**0.83**	**0.93***	
	p-value	0.053	<.0001	0.109	0.006	0.015	0.189	0.133	0.374	0.249	0.010	0.011	0.001	
	n	8	8	7	7	5	4	8	6	8	8	8	8	
CMBtp			**0.81**	**0.91**	**0.90**	0.92	0.86	**0.91**	−0.57	0.66	**0.90**	**0.90**	**0.72**	
			0.015	0.004	0.006	0.028	0.136	0.002	0.240	0.077	0.003	0.002	0.042	
			8	7	7	5	4	8	6	8	8	8	8	
CMBck				0.73	**0.95**	**0.96**	0.88	**0.71**	−0.46	0.51	**0.91**	**0.91**	**0.94**	
				0.063	0.001	0.011	0.122	0.048	0.361	0.195	0.002	0.002	0.001	
				7	7	5	4	8	6	8	8	8	8	
UMD					**0.83**	**0.91**	0.77	**0.79**	−0.74	0.71	**0.79**	0.75	0.75	
					0.021	0.032	0.226	0.034	0.094	0.071	0.033	0.050	0.053	
					7	5	4	7	6	7	7	7	7	
PM1						**0.97**	0.91	**0.90**	−0.39	0.79	**0.93**	**0.95**	**0.88**	
						0.006	0.093	0.006	0.451	0.033	0.003	0.001	0.009	
						5	4	7	6	7	7	7	7	
pDRc							−1	0.79	−0.90	0.82	0.94	**0.88**	0.90	
								0.114	0.099	0.092	0.020	0.048	0.037	
							2	5	4	5	5	5	5	
AE								0.94	−0.04	0.40	0.93	0.95	0.91	
								0.060	0.962	0.599	0.067	0.046	0.091	
								4	4	4	4	4	4	

	PMck	CMBtp	CMBck	UMD	PM1	pDRc	AE	Acu	PT	PAS	PAH	EC-TOR	OC-TOR
Acu									−0.30	0.69	0.89	**0.93**	0.63
									0.569	0.056	0.003	0.001	0.096
									6	8	8	8	8
PT										−0.40	−0.54	−0.36	−0.55
										0.438	0.264	0.485	0.258
										6	6	6	6
PAS											0.69	0.66	0.50
											0.059	0.075	0.208
											8	8	8
PAH												**0.97**	**0.84**
												<.0001	0.009
												8	8
EC-TOR													**0.84**
													0.010
													8

*Pearson r=0.97 after discarding an outlier for OC4 (28 μg/m^3) in the forward run 3 of Bus 1

Atmos Environ. Author manuscript; available in PMC 2011 September 1.